First Observation of Nonreciprocal X-Ray Gyrotropy

J. Goulon, A. Rogalev, C. Goulon-Ginet, G. Benayoun, and L. Paolasini
European Synchrotron Radiation Facility (ESRF), Boîte Postale 220, 38043 Grenoble Cedex, France

C. Brouder and C. Malgrange
Universités Paris-VI et VII, Laboratoire de Minéralogie-Cristallographie associé au CNRS, 4 place Jussieu, F-75252 Paris Cedex 05, France

P. A. Metcalf
Department of Chemistry, Purdue University, West Lafayette, Indiana 47907
(Received 30 May 2000)

We report the first observation of a *nonreciprocal* x-ray linear dichroism caused by the time-reversal odd, *real* part ζ of the complex gyrotropy tensor ζ^* which is dominated by electric dipole-electric quadrupole $E1E2$ interference terms. A nonreciprocal transverse anisotropy was observed in the low temperature insulating phase of a Cr doped V_2O_3 Mott crystal when a *single* antiferromagnetic domain was grown by magnetoelectric annealing along the hexagonal **c** axis. This new element (edge) specific spectroscopy could nicely complement x-ray magnetic circular dichroism which is silent for *antiferromagnetic* materials.

PACS numbers: 78.70.Dm, 75.80.+q, 78.20.Ls

X-ray *natural* circular dichroism (XNCD), i.e., a differential absorption of left- and right-handed circularly polarized x-ray photons, has long been expected in systems whose symmetry belongs to a subset of the *proper* rotation groups (C_n, D_n) or, under restrictive geometric conditions, to selected low symmetry groups (C_{2v}, D_{2d}, S_4, C_s) containing reflection planes. Very recently, XNCD was finally observed in various noncentrosymmetrical crystals satisfying these symmetry criteria [1–4]. In this Letter, we are concerned with a *nonreciprocal* x-ray linear dichroism (XLD), i.e., the differential absorption of the (σ, π) components of linearly polarized x-ray photons: such a dichroism should show up in crystals in which inversion symmetry is again broken, but now as a consequence of some *magnetic ordering*. Since this magnetic order is typically antiferromagnetic, such crystals cannot exhibit any Faraday rotation or any magnetic circular dichroism in the x-ray range. The link between XNCD and nonreciprocal XLD is a complex *gyrotropy tensor* $\zeta - i\zeta'$ which, in the x-ray range, is dominated by electric dipole-electric quadrupole ($E1E2$) interference terms in Fermi's golden rule [5]. Natural optical activity refers to its *imaginary part* ζ' which is required to have an *even* time-reversal symmetry to induce differential light absorption [6]. In contrast, the *real part* ζ having *odd* time-reversal symmetry [6] is expected to cause *nonreciprocal effects* in magnetic crystals of appropriate symmetry. Whereas *nonreciprocal birefringence* [7–12] was predicted to be a small effect at optical wavelengths, we point out below that *nonreciprocal* XLD can be easily detected: a nonreciprocal transverse anisotropy was successfully detected in the insulating, low temperature phase of a Cr doped V_2O_3 Mott crystal when a *single* antiferromagnetic domain was grown by magnetoelectric annealing [13]. The symmetry properties of the magnetoelectric tensor of this crystal led us to apply simultaneously an electric and a magnetic field both oriented along the hexagonal **c** axis, whereas the magnetic moments are known to be rotated by 71°–75° with respect to the **c** axis [14–16]. Even though our experiment bears no direct implication regarding the important issue of orbital occupancy in filled states [17–19], *ab initio* simulations of nonreciprocal XLD spectra should help to cross-check the validity of existing theoretical models in noncentrosymmetrical magnetic systems.

For a transverse polarized wave propagating along the direction **n**, the complex scattering tensor $a^\star_{\alpha\beta}$ can be expanded as [6,20,21]

$$a^\star_{\alpha\beta} = \alpha^\star_{\alpha\beta} + \zeta^\star_{\alpha\beta\gamma} \cdot n_\gamma + Q^\star_{\alpha\gamma\gamma\beta} \cdot [n^2_\gamma] + \cdots . \tag{1}$$

Here $\alpha^\star_{\alpha\beta}$ and $Q^\star_{\alpha\gamma\gamma\beta}$ (with $\alpha, \beta \neq \gamma$) are the complex electric dipole ($E1$) and electric quadrupole ($E2$) *polarizability* tensors. The real and imaginary parts of the gyrotropy tensor $\zeta^\star_{\alpha\beta\gamma} = \zeta_{\alpha\beta\gamma} - i\zeta'_{\alpha\beta\gamma}$ are related to *symmetric* and *antisymmetric* combinations of the $E1E2$ interference terms [6,11,20]:

$$A_{\alpha\beta\gamma}(f^\star) = \frac{2}{\hbar} \sum f^\star \omega^\star_{ij} \,\mathrm{Re}\{\langle i|E1_\alpha|j\rangle\langle j|E2_{\beta\gamma}|i\rangle\}, \tag{2a}$$

$$A'_{\alpha\beta\gamma}(f^\star) = -\frac{2}{\hbar} \sum f^\star \omega^\star_{ij} \,\mathrm{Im}\{\langle i|E1_\alpha|j\rangle\langle j|E2_{\beta\gamma}|i\rangle\} \tag{2b}$$

with

$$\zeta_{\alpha\beta\gamma} = \zeta_{\beta\alpha\gamma} = \tfrac{\omega}{3c}[A'_{\alpha\beta\gamma} + A'_{\beta\alpha\gamma}],$$

$$\zeta'_{\alpha\beta\gamma} = -\zeta'_{\beta\alpha\gamma} = \tfrac{\omega}{3c}[A_{\alpha\beta\gamma} - A_{\beta\alpha\gamma}].$$

Since the amplitude of $\zeta^\star$ is proportional to ω, one expects the gyrotropy tensor to become quite significant in x-ray spectroscopy. Near resonance, linear and circular dichroisms are given by [21]

$$\begin{aligned} \sigma^\pi - \sigma^\sigma &\propto [\alpha_{xx} - \alpha_{yy}] + [\zeta_{xxz} - \zeta_{yyz}] \\ &\quad + [Q_{xzzx} - Q_{yzzy}], \\ \sigma^L - \sigma^R &\propto 2\{\alpha'_{xy} + \zeta'_{xyz} + Q'_{xzzy}\}. \end{aligned} \tag{3}$$

The *real* and *imaginary* parts of the electric polarizability tensors $\alpha^\star$ and $Q^\star$ have, respectively, even and odd time-reversal symmetry whereas the real and imaginary parts of the gyrotropy tensor have again *the opposite time-reversal symmetry.* Thus, $\{\alpha'_{xy} + Q'_{xzzy}\}$ are easily identified as the terms which contribute to x-ray magnetic circular dichroism (XMCD), whereas ζ'_{xyz} contributes to XNCD. Similarly, the first and last terms in Eq. (3) contribute to natural linear dichroism if a crystal exhibits a structural anisotropy in a plane perpendicular to the wave vector $\mathbf{k}$; in magnetic crystals, the second term $[\zeta_{xxz} - \zeta_{yyz}]$ may also contribute to a *transverse nonreciprocal* XLD the sign of which will depend whether the *axial* ordering magnetic field is *parallel* or *antiparallel* with $\mathbf{k}$. Only 13 noncentrosymmetric crystal classes have a nonvanishing imaginary part of the x-ray gyrotropy tensor ζ'_{xyz} and can exhibit XNCD [1–4]. To identify which crystal may exhibit nonreciprocal XLD, one should simply remember that nonreciprocal gyrotropy and the magnetoelectric effect are closely related. This was first perceived by Birss and Shrubsall [8] and clarified by Hornreich and Shtrikman [9] who pointed out the importance of the $E1E2$ interference terms. More recently, Graham and Raab [11] refined the theory of Hornreich and Shtrikman. There are 58 noncentrosymmetric magnetic crystal classes that are magnetoelectric [22]. The generic example is Cr_2O_3 that has the centrosymmetric corundum structure (space group $R\bar{3}c$) but the noncentrosymmetric $\underline{\bar{3}m}$ *space-time* group below the Néel temperature. In Cr_2O_3, the easy magnetization direction is along the trigonal axis and the magnetoelectric effect measured along the direction of the magnetic moments ($\alpha_\parallel$) is bigger than in any direction perpendicular to the moments ($\alpha_\perp$). Obviously, in such a *uniaxial* magnetic crystal, a magnetoelectric effect *parallel* to the hexagonal $\mathbf{c}$ axis cannot induce any anisotropy in the *perpendicular* basal plane. This was confirmed experimentally. The situation is, however, more propitious in the antiferromagnetic insulator phase (AFI) of V_2O_3 below T_N: in this crystal, the magnetic moments ($1.2\mu_B$ per V atom) are rotated by 71° with respect to the hexagonal axis and time-inversion symmetry is broken in the magnetic group $A2$ [15,16] which, according to Birss [22], is magnetoelectric. Since the first order phase transition from the trigonal paramagnetic phase (space group $R\bar{3}c$) to the monoclinic AFI low temperature phase (space group $I2/a$) turns out to be crystal destructive, Cr-doped crystals $(V_{1-x}Cr_x)_2O_3$ are usually preferred for temperature dependent magnetic and structural studies [23–26]. Here, we reused the same crystal as for previous resonant x-ray scattering experiments carried out at the European Synchrotron Radiation Facility (ESRF) (beam line ID20) [26]: this Cr-doped crystal ($1.0 \times 0.8 \times 0.05$ mm^3) was cleaved perpendicular to the hexagonal $\mathbf{c}$ axis. With $x = 0.028$, not only T_N raises from 150 to ca. 181 K, but also the electric resistivity is substantially increased in the paramagnetic phase. Magnetoelectric annealing [14,27] initiated in the paramagnetic insulating phase was exploited to generate a *single antiferromagnetic domain:* we applied simultaneously along the direction of the hexagonal $\mathbf{c}$ axis a modest electric field (5×10^3 V/cm) plus a weak magnetic field (± 0.5 T), the two fields being either *parallel* or *antiparallel*. Next, the crystal was cooled down below the phase transition and the electric field was ultimately switched off during the XLD experiment. Note that the crystal was systematically heated up to 300 K, i.e., back in the paramagnetic phase, before we inverted the direction of the magnetic field and repeated the whole magnetic annealing procedure.

All spectra were recorded at the ESRF beam line ID12A [28]. For XLD experiments, the source was a helical undulator (Helios-II) emitting circularly polarized x-ray photons: a diamond phase plate located after the Si(111) double crystal monochromator was used to convert the circularly polarized photons into (σ, π) linearly polarized photons and to switch quickly from one linear polarization to the orthogonal one. For XNCD experiments, a new electromagnetic helical undulator [29] allowed us to flip the helicity of the x-ray photons several times for each energy data point. Fluorescence detected dichroism spectra [21] were recorded in the backscattering configuration, the detector being directly inserted inside the cryomagnet containing the sample. All x-ray fluorescence spectra were carefully corrected for reabsorption.

We have reproduced in Fig. 1 the V K-edge x-ray appearance near-edge structure (XANES) and XLD spectra recorded in the trigonal phase $R\bar{3}c$ *before* magnetoelectric annealing. In our deconvolved XANES spectrum, the pre-edge shoulders labeled "B" and "C" by Bianconi and Natoli [30] are now nicely resolved peaks separated by 1.65 eV: these resonances were assigned to final states involving the $3d$ metal orbitals featuring the usual T_{2g} and E_g symmetry in an octahedral crystal field with $10Dq$ energy splitting. The degeneracy of the T_{2g} level is further lifted by the trigonal ligand field (D_{3d}): the corresponding energy splitting into e_g and a_{1g} sublevels is small and should not be observed in the K-edge XANES spectrum because transitions to the fully symmetrical a_{1g} sublevel are forbidden by $E1$ and $E2$ selection rules or the crystal

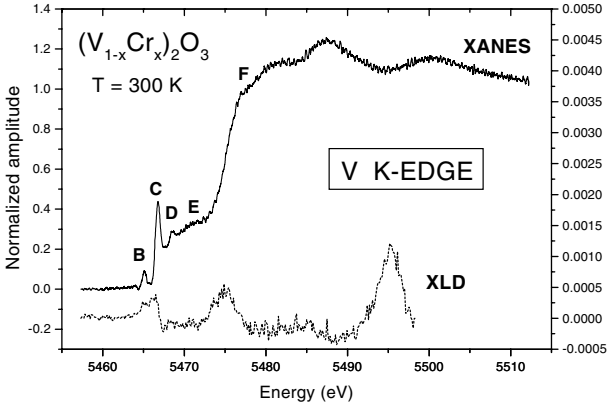

FIG. 1. Deconvolved XANES and weak XLD spectra in the paramagnetic phase of $(V_{1-x}Cr_x)_2O_3$. The x-ray wave vector **k** was collinear with the hexagonal **c** axis.

orientation. The weak prepeak *B* should therefore be most probably assigned to final states involving the e_g orbitals of the metal, such transitions having implicitly a strong *E*2 character. As expected, there is only a very weak linear dichroism signal ($\leq 3 \times 10^{-4}$) in the pre-edge region: we cannot exclude yet the fact that it may result from a small misalignment of the crystal axis with respect to the wave vector **k**.

The XLD spectra recorded in the AFI phase *after magnetoelectric annealing* are displayed in Fig. 2: their amplitude is spectacularly increased, the maximum intensity being now of the order of ca. 1%. As expected for a *time-reversal odd* effect, the sign of the dichroism is nicely inverted when the direction of the magnetic field used during the magnetoelectric annealing is inverted with respect to the electric field. Figure 2 thus produces the demonstration that our experiment is different from a conventional, uniaxial x-ray magnetic linear dichroism (XMLD) experiment [31–34] in which a magnetic anisotropy is typically created by a magnetic field rotated by 90° with respect to

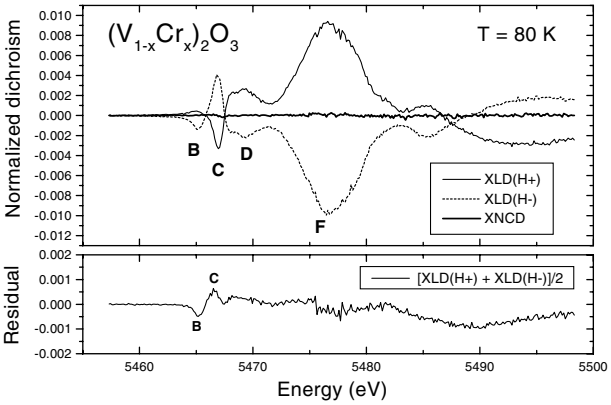

FIG. 2. Nonreciprocal XLD spectra recorded in the monoclinic phase. Magnetoelectric annealing was performed with parallel (+) and antiparallel (−) electric and magnetic fields. The XNCD spectrum displayed at the same scale is hardly visible. The residual signal $XLD(H^+) + XLD(H^-)$ is displayed with an expanded scale.

the wave vector **k**: in the latter experiment, the XMLD signal is proportional to $\langle M^2 \rangle$ and remains *unchanged* when the direction of the magnetic field is inverted. A careful comparison of Figs. 1 and 2 would reveal that the peak locations and the line shapes are quite different in the XLD spectra recorded at high and low temperature. Interestingly, the nonreciprocal XLD signal measured at the pre-edge resonance *B* is rather small in comparison with the XLD signal measured at the pre-edge resonance *C*: remember that the former resonance was assigned to transitions towards the partially populated levels e_g (possibly involved in *orbital ordering* models [17–19]) whereas resonance *C* was assigned to transitions towards final states involving metal orbitals of symmetry E_g. It should also be kept in mind that the observation of an $E1E2$ gyrotropy signal implies a substantial *parity mixing* between $3d$ and $4p$ metal orbitals: this is most favorable in the case of the empty E_g orbitals which are strongly hybridized with the ligand orbitals. This is not the case for the e_g orbitals which are more sensitive to metal-metal exchange interactions and we expect the peak *B* to keep a strong *E*2 character. Nevertheless, even peak *B* exhibits a marked *anisotropy* and this could perhaps give indirectly some quantitative information about the orbital occupancy problem. At this stage, it is not obvious why the sign of the nonreciprocal anisotropy is inverted for bands *B* and *C*, respectively. On the other hand, we observe a strong nonreciprocal XLD signal at all resonance involving the $4p$-$5p$ metal orbitals: this is in full agreement with the magnetic scattering experiments reported in Ref. [26]. In contrast with the erroneous idea that the electric quadrupole *E*2 transition would exist only in the pre-edge region, it clearly appears that the nonreciprocal gyrotropy spectrum extends (at least) over the whole XANES region. Whether or not the signal could extend further into the extended x-ray-absorption fine structure regime is still an open question. Note that there are small but significant differences between the XLD^+ and XLD^- spectra: the weak residual signal associated with their half sum (see Fig. 2) could perhaps be assigned to a (time-even) linear dichroism due to the slightly distorted monoclinic structure (space group $I2/a$).

Although the *local* point group *C*3 at each metal center is chiral, the space group $I2/a$ belongs to a centrosymmetric crystal class $(2/m)$ for which *no* XNCD should ever be observed (point group C_{2h}). We tried nevertheless to record the XNCD spectrum (without any magnetic/electric field): as illustrated by Fig. 2 there is only an extremely weak residual signal ($\leq 1.5 \times 10^{-4}$). Its fairly low intensity calls for the conclusion that the monoclinic structure does not exhibit any marked deviation from a centrosymmetric structure, even after magnetoelectric annealing. In contrast, the huge *nonreciprocal* gyrotropy signals of Fig. 2 confirm that the noncentrosymmetry has *only* a magnetic origin.

In the one-electron transition picture, the photoionized $1s$ level has no spin-orbit coupling and a spin dependence

of the absorption process can be induced only by spin-orbit coupling in the final state, the spectra becoming sensitive to spin-polarization effects by exchange interactions. As in the case of XMCD spectra of ferromagnetic systems, we expect the orbital angular momentum $\langle \mathbf{L} \rangle$ to play a key role in nonreciprocal XLD spectra. One may hope to learn more about orbital occupancy in filled states by exploiting *sum rules* as this is classically done for XMCD spectra [35]. Recall that sum rules have already been derived for XNCD, i.e., for the imaginary part of the gyrotropy tensor [5] and their extension to the real part was recently attempted [36]. An important outcome of this new theory was to show that $\langle \mathbf{L} \rangle$ *is not a suitable operator* for describing the electronic and magnetic properties of noncentrosymmetric antiferromagnetic crystals: more sophisticated operators are needed.

Nonreciprocal XLD should indeed nicely complement *nonreciprocal* second harmonic generation (SHG) which emerged recently as a valuable method to characterize antiferromagnetic materials at optical wavelengths [37]. Note that nonreciprocal XLD is probing $E1E2$ interference terms which becomes quite significant in the x-ray range, whereas nonreciprocal SHG is still probing electric dipole-magnetic dipole ($E1M1$) interference terms. Moreover, nonreciprocal XLD benefits of the advantage to be element and edge specific as any x-ray spectroscopy.

The authors are grateful to C. R. Natoli, P. Carra, and F. Sette for their comments and fruitful discussions. The crystal was grown in the Chemistry Department of Purdue University.

[1] J. Goulon, C. Goulon-Ginet, A. Rogalev, V. Gotte, C. Malgrange, C. Brouder, and C. R. Natoli, J. Chem. Phys. **108**, 6394 (1998).
[2] L. Alagna, T. Prosperi, S. Turchini, J. Goulon, A. Rogalev, C. Goulon-Ginet, C. R. Natoli, R. D. Peacock, and B. Stewart, Phys. Rev. Lett. **80**, 4799 (1998).
[3] J. Goulon, C. Goulon-Ginet, A. Rogalev, V. Gotte, C. Malgrange, and C. Brouder, J. Synchrotron Radiat. **6**, 673 (1999).
[4] J. Goulon, C. Goulon-Ginet, A. Rogalev, G. Benayoun, C. Brouder, and C. R. Natoli, J. Synchrotron Radiat. **7**, 182 (2000).
[5] C. R. Natoli, C. Brouder, Ph. Sainctavit, J. Goulon, C. Goulon-Ginet, and A. Rogalev, Eur. Phys. J. B **4**, 1 (1998).
[6] L. D. Barron, in *Molecular Light Scattering and Optical Activity* (Cambridge University Press, Cambridge, England, 1982).
[7] W. F. Brown, S. Shtrikman, and D. Treves, J. Appl. Phys. **34**, 1233 (1963).
[8] R. R. Birss and R. G. Shrubsall, Philos. Mag. **15**, 687 (1967).
[9] R. M. Hornreich and S. Shtrikman, Phys. Rev. **171**, 1065 (1968).
[10] R. V. Pisarev, Sov. Phys. JETP **31**, 761 (1970).
[11] E. B. Graham and R. E. Raab, Philos. Mag. **66**, 269 (1992).
[12] B. B. Krichevtsov, V. V. Pavlov, R. V. Pisarev, and V. N. Gridnev, J. Phys. Condens. Matter **5**, 8233 (1993).
[13] O. F. De Alcantara Bonfim and G. A. Gehring, Adv. Phys. **29**, 731 (1980).
[14] R. M. Moon, Phys. Rev. Lett. **25**, 527 (1970).
[15] W. B. Yelon, S. A. Werner, R. E. Word, J. M. Honig, and S. Shivashankar, J. Appl. Phys. **52**, 2237 (1981).
[16] R. E. Word, S. A. Werner, W. B. Yelon, J. M. Honig, and S. Shivashankar, Phys. Rev. B **23**, 3533 (1981).
[17] C. Castellani, C. R. Natoli, and J. Ranninger, Phys. Rev. B **18**, 4945 (1978).
[18] M. Fabrizio, M. Altarelli, and M. Benfatto, Phys. Rev. Lett. **80**, 3400 (1998); **81**, 4030(E) (1998).
[19] J. H. Park, L. H. Tjeng, A. Tanaka, J. W. Allen, C. T. Chen, P. A. Metcalf, J. M. Honig, F. M. F. de Groot, and G. A. Sawatzky, Phys. Rev. B **61**, 11 506 (2000).
[20] A. D. Buckingham, Adv. Chem. Phys. **12**, 107 (1967).
[21] J. Goulon, C. Goulon-Ginet, A. Rogalev, V. Gotte, C. Brouder, and C. Malgrange, Eur. Phys. J. B **12**, 373 (1999).
[22] R. R. Birss, *Symmetry and Magnetism,* in Selected Topics in Solid State Physics, edited by E. P. Wohlfarth (North-Holland, Amsterdam, 1966), Vol. III.
[23] D. B. McWhan and J. P. Remeika, Phys. Rev. B **2**, 3734 (1970).
[24] A. Menth and J. P. Remeika, Phys. Rev. B **2**, 3756 (1970).
[25] P. D. Dernier and M. Marezio, Phys. Rev. B **2**, 3771 (1970).
[26] L. Paolasini, C. Vettier, F. de Bergevin, F. Yakhou, D. Mannix, A. Stunault, W. Neubeck, M. Altarelli, M. Fabrizio, P. A. Metcalf, and J. M. Honig, Phys. Rev. Lett. **82**, 4719 (1999).
[27] T. H. O'Dell, *The Electrodynamics of Magnetoelectric Media,* in Selected Topics in Solid State Physics, edited by E. P. Wohlfarth (North-Holland, Amsterdam, 1970), Vol. XI.
[28] J. Goulon, A. Rogalev, C. Gauthier, C. Goulon-Ginet, S. Pasté, R. Signorato, C. Neumann, L. Varga, and C. Malgrange, J. Synchrotron Radiat. **5**, 232 (1998).
[29] A. Rogalev, J. Goulon, G. Benayoun, P. Elleaume, J. Chavanne, Ch. Penel, and P. Van Vaerenbergh, Proc. SPIE Int. Soc. Opt. Eng. **3773**, 275 (1999).
[30] A. Bianconi and C. R. Natoli, Solid State Commun. **27**, 1177 (1978).
[31] G. van der Laan, B. T. Thole, G. A. Sawatzky, J. B. Goedkoop, J. C. Fuggle, J.-M. Esteva, R. Karnatak, J. P. Remeika, and H. A. Dabkowska, Phys. Rev. B **34**, 6529 (1986).
[32] D. Alders, L. H. Tjeng, F. C. Voogt, T. Hibma, G. A. Sawatzky, C. T. Chen, J. Vogel, M. Sacchi, and S. Iacobucci, Phys. Rev. B **57**, 11 623 (1998).
[33] J. Stöhr, A. Scholl, T. J. Regan, S. Anders, J. Lūning, M. R. Scheinfein, H. A. Padmore, and R. L. White, Phys. Rev. Lett. **83**, 1862 (1999).
[34] G. Van der Laan, J. Magn. Magn. Mater. **192**, 297 (1999).
[35] B. T. Thole, P. Carra, F. Sette, and G. Van der Laan, Phys. Rev. Lett. **68**, 1943 (1992).
[36] P. Carra and R. Benoist, Phys. Rev. B **62**, R7703 (2000).
[37] M. Fiebig, D. Fröhlich, B. B. Krichevtsov, and R. V. Pisarev, Phys. Rev. Lett. **73**, 2127 (1994).